ORIGINAL ARTICLE

Characterization of a low cost *Lagenaria vulgaris* based carbon for ranitidine removal from aqueous solutions

CrossMark

Danijela Bojić [a], Milan Momčilović [b],*, Dragan Milenković [c], Jelena Mitrović [a], Predrag Banković [d], Nena Velinov [a], Goran Nikolić [e]

[a] *University of Niš, Department of Chemistry, Faculty of Science and Mathematics, 33 Višegradska St., 18000 Niš, Serbia*
[b] *University of Belgrade, Institute of Nuclear Sciences "Vinča", P.O. Box 522, 11001 Belgrade, Serbia*
[c] *High Chemical Technological School, 36 Kosančićeva St., 37000 Kruševac, Serbia*
[d] *University of Belgrade, Institute of Chemistry, Technology and Metallurgy, Center for Catalysis and Chemical Engineering, 12 Njegoševa St., 11000 Belgrade, Serbia*
[e] *University of Niš, Faculty of Technology, 124 Bulevar oslobođenja St., 16000 Leskovac, Serbia*

Abstract Practical aspects of *Lagenaria vulgaris* shell conversion to activated carbon were examined along with its use in ranitidine adsorption. Kinetics and isotherms of adsorption onto *Lagenaria vulgaris* carbon (LVC) were correlated to several theoretical adsorption models. The best fit was found in the case of Langmuir and pseudo-second-order model indicating monolayer adsorption. The influence of pH under kinetic study showed slightly hindered adsorption below pH 4. The optimal adsorbent dosage was set to 1 g/L. LVC was characterized by several complementary techniques, including wet chemical techniques such as Boehm's titrations and determination of pH_{PZC} and pH of LVC, which revealed neutral nature of the adsorbent. N_2 sorptometry determined specific surface area of 665 m^2/g and significant ratio of micropores in the sample with maximum wall's diameter of 2.2 nm. Fourier transform infrared spectroscopy (FTIR) confirmed the role of lignin and cellulose in the formation of the final LVC structure. Porous structure of the material was proved by using scanning electron microscopy. Preparation of LVC material drew attention as an easy and low-cost process for production of a highly efficient adsorbent which

* Corresponding author.
E-mail address: milanmomcilovic@yahoo.com (M. Momčilović).
Peer review under responsibility of King Saud University.

ELSEVIER **Production and hosting by Elsevier**

exhibited fast kinetics of ranitidine removal in the first minutes of contacting and large adsorption capacity (315.5 mg/g) at equilibrium.

1. Introduction

It has been shown that Ranitidine is one of the most popular drugs on the planet used on daily base due to frequent gastric problems in humans today. It is manufactured in tons annually and easily incorporated in spontaneous mechanism of environmental pollution, especially in urban areas. Ranitidine is being excreted by urine and feces, parent compound or metabolites reach the sewage system, wastewater treatment plant remove them only partially (Jones et al., 2005), so it eventually ends up in surface water, mainly rivers. In addition, unwanted or expired ranitidine doses are disposed from households and hospitals on daily basis directly to the sewage systems. In the study conducted in Italy, ranitidine was identified in a group of pharmaceuticals with a "priority" for the environment (Castiglioni et al., 2006). This group encounters daily loads of 50–500 mg for 1000 inhabitants in the influents and estimated residual loads, while after its removal in sewage treatment plants and in the river it drops to 25–280 mg for 1000 inhabitants daily, which results from 1.5 to 16 kg/day if we extrapolate this data to the whole of Italy. Its overall presence in water bodies all over the world is significant.

Ranitidine (Fig. 1) is a histamine H_2 receptor antagonist which is prescribed for the treatment of duodenal and gastric ulceration since it efficiently decreases the amount of acid produced in the stomach (Pfaffen and Ortiz, 2010). Ranitidine is a furan derivative, with a nitroenamine urea polar group and dimethylamine group enhancing the basic character of its heterocyclic moiety. It is metabolized by demethylation, N- and S-oxidation, but after oral administration, about 30–70% of it is eliminated unchanged in urine within 24 h (Vediappan and Lee, 2011).

Pharmaceuticals cannot be absolutely removed in sewage treatment plants using conventional techniques such as bioremediation and physicochemical treatments, including coagulation, volatilization, sedimentation and filtration (Sires and Brillas, 2012). On the other hand, adsorption has shown promising results. Up to now, adsorption of various drugs onto zeolites (Fukahori et al., 2011), chitosan (Kyzas et al., 2013), clays (Figueroa et al., 2004) and activated carbons prepared from different residues (Cabrita et al., 2010) was reported. Photoassisted degradation of many pollutants, including ranitidine, is an efficient technique, but it deserves special plants and expensive equipment (Addamo et al., 2005).

Powdered and granular activated carbons are considered the most potent adsorbents used commercially. However, they are expensive (Salleha et al., 2011) which imposes the need for searching a cheaper preparation procedures or precursors. Importantly, the resulting properties of the carbon depend on the used precursor (Menendez-Diaz and Martin-Gullon, 2006). Recently, many interesting alternatives have been proposed in the scientific literature, including preparation of activated carbons from livestock sewage sludge (Wu et al., 2014), aguaje and olive fruit stones (Obregón-Valencia and Rosario Sun-Kou, 2014), reedy grass leaves (Xu et al., 2014), orange peel (Fernandez et al., 2014), Golden Bamboo (González and Pliego-Cuervo, 2014), and marigold straw (Qin et al., 2014). The main goal of such studies is to examine the possibilities for producing novel and cheaper forms of carbon adsorbents with standard or even better properties.

We examined activated carbon derived from *Lagenaria vulgaris* as a suitable adsorbent for the small scale ranitidine adsorption under laboratory conditions. *L. vulgaris* is a climbing, hardy plant mainly grown on alluvial sandy soil and it belongs to the family *Cucurbitaceae*. Although it has a wide medicinal use (Ghule et al., 2009), it is mainly used as a container for water and food worldwide, known as "The Bottle Gourd" (Decker-Walters et al., 2004). The outer shell of the plant is composed of lignin and cellulose (Mitić-Stojanović et al., 2012). Such structure is recognized as one of the key features in production of activated carbons.

The goal of this study was to examine practical options for conversion of *L. vulgaris* to activated carbon and its possible use in ranitidine removal by adsorption from contaminated water sources. Kinetics, isotherms, effect of pH of ranitidine adsorption and adsorbent dosage of LVC were investigated under batch conditions. Detailed characterization of adsorbent was performed in order to acquire as much information as possible about its structure and reactivity.

2. Materials and methods

2.1. Adsorbent preparation

Carbon adsorbent was derived from *L. vulgaris* shell by the thermo-chemical procedure. Initially, the dried fruit was rinsed with tap and then demineralized water in order to remove dust and soil from it. Small pieces of broken shell were manually
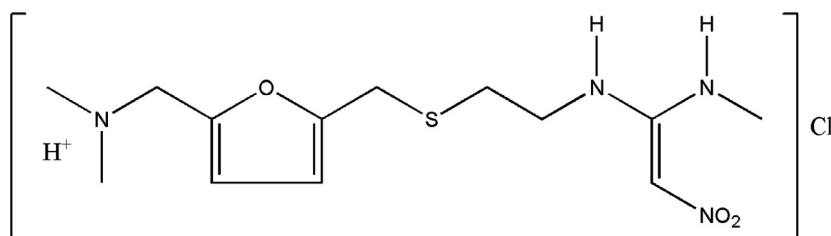
Figure 1 Molecular structure of ranitidine hydrochloride.

separated from the inner fruit and rinsed and milled in demin-eralized water, filtered, dried at 55 °C and finally fractionized using several sieves (Endecotts, England). The biomass with granulation of 0.8–1.25 mm was further immersed in 10% H$_2$SO$_4$ (Merck, Germany) and stirred occasionally within 48 h. The obtained material was rinsed with distilled water until neutral pH and dried at room temperature overnight and then at 105 °C for 24 h. Such substrate was carbonized in tubular furnace under the protective atmosphere of nitrogen by heating from room temperature to 400 °C with gradient 3 °C/min. Material was held 60 min at 400 °C and then acti-vated in steam (110 mL/min) by increasing temperature to 700 °C with gradient 3 °C/min. After another hour at 700 °C, furnace was spontaneously cooled down in inert atmosphere. The obtained material was rinsed with demineralized water, dried at 105 °C for 2 h and stored in a closed bottle.

2.2. Instrumentation

Textural properties were analyzed from nitrogen isotherms measured at −196 °C using Sorptomatic 1990 (Thermo Fisher Scientific, USA). Prior to experiment, the sample was out-gassed under a reduced atmosphere at 160 °C for 20 h. The isotherms were used to calculate the specific surface area by the BET method with two parameters line (S_{BET}) (Brunauer et al., 1938). Micropore volume was calculated by Dubinin–Radushkevich model (V_{mic}) (Rouquerol et al., 1999), while Barret–Joyner–Halenda method was used for mesopore and pore size distribution (PSD) analysis (Barrett et al., 1951). Maximum pore diameter (d_{max}) was determined from the same plot.

Fourier transform infrared spectroscopy (FTIR) analysis was used to detect same peaks characteristic for carbons. FTIR spectrometer BOMEM MB-100 (Hartmann & Braun, Canada) was operated in spectral range 4000–400 1/cm with resolution of 2 1/cm. Two samples, non-carbonized *L. vulgaris* shell and LVC were compressed in a potassium bromide (KBr) pellet prior to spectroscopy.

The surface micrographs of LVC were taken by using a scanning electron microscope JSM-6610LV (Jeol, USA). Sample was pretreated by gold sputtering in order to increase conductivity and fixate tiny surface particles for better imaging.

Residual ranitidine concentrations were determined by spectrophotometer Shimadzu UV–vis 1650 PC (Shimadzu, Japan) at 313 nm with detection limit 1 mg/mL (Salve et al., 2010). For determination of low ranitidine concentrations spectrophotometric method, based on addition of ceric ammo-nium sulfate and dye crystal violet with measuring absorbance at 582 nm was applied (detection limit 0.1 mg/L (Narayana et al., 2010).

2.3. Chemicals and reagents

A 1000 mg /L stock solution of ranitidine hydrochloride (C$_{13}$H$_{22}$N$_4$O$_3$S·HCl; Mr = 350.87 g/mol) was prepared by dissolv-ing the measured amount of white granular substance in distilled water. Ranitidine purchased from Sigma–Aldrich (St. Louis, MO, USA) was >99% in purity. This stock solu-tion was used for preparing a series of drug concentrations ranging from 10 to 400 mg/L.

2.4. Determination of pH$_{PZC}$

Drift method was used for the determination of pH$_{PZC}$ in 0.1 M NaNO$_3$ solution as inert electrolyte. For this method, series of 100 mL electrolyte solutions were adjusted to various pH values, approximately at 2, 3, 4, 5, 6, 7, 8, 9 and 10 using 0.1/0.01 M HNO$_3$ and/or NaOH. These pH values were declared as initial (pH$_i$). Then, 0.2 g of LVC samples was added to each solution, sealed and stirred overnight. After that, measured pH values of suspensions were declared as final (pH$_f$). A plot with dependence of pH$_f$ from pH$_i$ was used to determine pH$_{PZC}$ as the point of interception between the dotted curve and diagonal at the plot.

2.5. Boehm's titrations

Boehm's titrations were used to determine the extent of vari-ous oxygen acidic functional groups (Ofomaja and Naidoo, 2010). Technique was carried out by using 0.01/0.1 M solu-tions of bases of growing ionic forces (NaHCO$_3$, Na$_2$CO$_3$ and NaOH). Initially, 0.5 g of LVC was protonated by mixing it with 0.01 M HCl during 1.5 h. This sample was drained, dried at 40 °C and suspended in 100 mL of 0.1 M NaNO$_3$. When pH became stable, the selected base was added in small portions (0.05 and 0.1 mL) waiting for stabilization of pH after every increment. During the procedure, nitrogen was intro-duced into the suspension in order to avoid the influence of atmospheric carbon-dioxide.

2.6. pH of LVC determination

pH of LVC was determined simply by suspending 0.5 g of adsorbent in 125 mL of demineralized water. After a couple of minutes stirring pH value was measured by pH-meter.

2.7. Adsorption experiments

The adsorption experiments were carried out by contacting 0.25 g of carbon adsorbent with 250 mL of ranitidine solution (adsorbent dosage = 1 g/L) in the sealed Erlenmeyer flasks stirred at 250 rpm and 25 °C maintained using a tempera-ture-controlled water bath. Initial ranitidine concentrations of 10, 20, 50, 100, 200, 300, and 400 mg/L were contacted with LVC and analyzed for residual concentrations after defined time intervals during 24 h. The native pH values of solutions were from 5 to 6.2 and were not additionally adjusted during the treatment.

Within the kinetic experiments, aliquots of 4 mL were withdrawn from the batch solution in defined intervals (1–1440 min), centrifuged, filtered using 0.45 μm regenerated cellulose membrane filter (Agilent Technologies, Germany), and determined for ranitidine using UV–vis technique. The adsorbed amount of ranitidine (q_e) was calculated out of differences of its initial (C_i) and residual concentration (C_t) after defined time, given by the Eq. (1):

$$q_e = \frac{(C_i - C_t)V}{m_{ads}} \tag{1}$$

where m_{ads} is the mass of adsorbent used (by Saad et al., 2014). Removal degree is calculated by:

$$R(\%) = \frac{(C_i - C_t)}{C_i} \times 100 \qquad (2)$$

For isotherm experiments, the same procedure and conditions were used. Contacting time of less than an hour was enough for reaching equilibrium. The adsorbed amount of ranitidine was plotted against its initial concentration in adsorption isotherm.

The effect of pH onto adsorption of ranitidine was examined within pH range from 2 till 11 for initial ranitidine concentration of 50 mg/L. Diluted NaOH and HCl solutions were used in drops for initial pH adjustments.

3. Results and discussion

3.1. Textural properties

N$_2$ adsorption/desorption isotherm for LVC given in Fig. 2(a) belongs to characteristic type IV which shows that adsorption/desorption processes do not follow the same way. An H$_2$-type
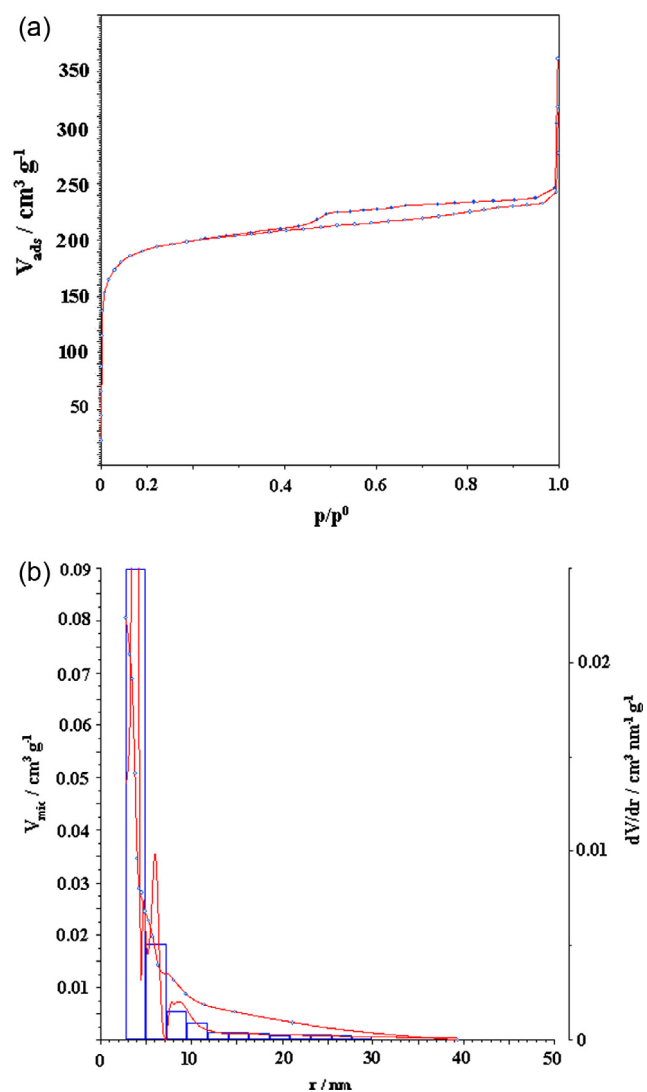
Table 1 Textural parameters of LVC.

S_{BET} (m^2/g)	V_{mic} (m^2/g)	S_{meso} (m^2/g)	V_{meso} (mL/g)	d_{max} (nm)
665	0.302	73	0.08	2.2

hysteresis loop corresponds to gas adsorption in the mesopores. Results obtained using gravimetric McBain method for adsorption/desorption isotherms of N$_2$ are given in Table 1. It is seen that LVC has relatively high BET surface area of 665 m^2/g which is probably due to well developed network of micropores. In addition, good gas adsorption at lower relative pressures indicates abundance of micropores. Pore size distribution obtained by applying Barret–Joyner–Halenda method (Fig. 2(b)) confirms a significant ratio of micropores in the sample where maximum wall's diameter equals 2.2 nm.

Acidification of raw precursor with sulfuric acid is acknowledged as important factor responsible for textural properties of obtained carbon (Aziz et al., 2009). Acids remove numerous metallic species absorbed during the growth of the plant which is significant for making oxygen functional groups available for other reactions including reactions that are taking part in adsorption mechanism. Sulfuric acid performs partial hydrolysis and activation of lignin and cellulose prior to heating, while during the heating carbonization is intensified. In addition, ash content in the carbons is reduced by acidic treatment (Youssef et al., 2004).

Wide comparison on textural properties of adsorbent and its adsorptive potential toward ranitidine removal is difficult to provide due to lack of background in the literature and studies similar to this. Mondala et al. (2014) described preparation of activated carbon from mung bean husk (MBH-SAC) with S_{BET} of 405 m^2/g and micro-pore volume was 0.2853 cm/g and this is similar to our case. However, MBH-SAC adsorption capacity of 28.0 mg/g is much lower than the capacity obtained in our work.

3.2. FTIR

FTIR spectra of the non-carbonized *L. vulgaris* shell and LVC are given in Fig. 3(a) and (b), respectively. FTIR spectrum of the *L. vulgaris* shell contains functional groups that are characteristic for cellulose (1000–1200 1/cm) and lignin (1200–1700 1/cm). Peaks at 1035, 1060, 1110, 1159 1/cm are typical for O—H, C—H, C—OH, C—O and CH$_2$ glycoside groups from cellulose. Main peaks identified at 1086, 1140, 1166 1/cm, and those at higher wave numbers (1221, 1269, 1326, 1367, 1423, 1464, 1510, 1596 1/cm) become from absorption of C—OH, C—H, CH$_2$, CH$_3$, C—O, and C=O groups (Rutherford et al., 2005). These peaks are used for the detection of structural changes during thermal treatment.

It can be noticed (Fig. 3) that carbonization induces lowering of intensity of several IR bands and shifting of their positions such as for cellulose groups (1030, 1105, 1160 1/cm) or even their diminishing in the case of lignin groups (1200–1500 1/cm). Decomposition of glycoside structure occurs. This fact is corroborated by the lowering of the intensity of the peaks at 3400 and 2900 1/cm typical for O—H and C—H stretching vibrations along with their deformation relatives.

During carbonization above 700 °C, the peaks of lower intensity gather in wide range reducing resolution and increas-
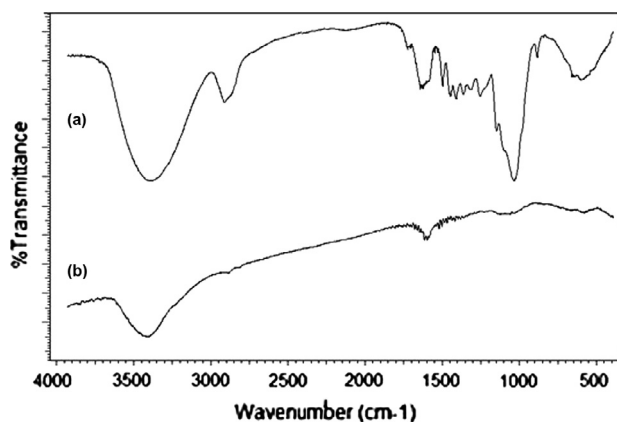

Figure 2 (a) Nitrogen adsorption/desorption isotherm for LVC and (b) pore size distribution.

Figure 3 FTIR spectra of (a) non-carbonized *Lagenaria vulgaris* shell and (b) LVC.

ing the noise (Fig. 3(b)). In such manner, lignin C=O band at 1700 1/cm which originate during carbonization, cannot be clearly noticed due to overlapping with wide lowered vibration of O—H at 1620 1/cm from crystal hydrate. Besides stretching vibration of O—H bond at 3400 1/cm, in the spectrum dominates the band at 1600 1/cm which comes from C=C vibrations of aromatic rings of lignin. Lowering the intensity of this band due to carbonization at 700 °C implies the formation of polycyclic structure which is expected to diminish at higher temperatures. Similar cases were described in the literature. Namely, during the treatment of the sample which contains lignin and cellulose at 400–500 °C, condensation of paraffin and aromatic structures occurs giving the similar IR spectrum (Rutherford et al., 2005). The presence of hydroxyl and carbonyl groups and aromatic compounds is an evidence of the lignocellulosic structure of *L. vulgaris* shell as also observed in other materials such as Brazilian coconut shell (Cazetta et al., 2011), coconut shell (Aljeboree et al., 2017) and jackfruit peel waste (Prahas et al., 2008).

3.3. Scanning electron microscopy (SEM)

SEM revealed that at micro-level LVC is mainly composed of tiny disorganized carbon crisps of various dimensions and diverse morphology. At Fig. 4(a) larger particle with porous structure is shown. It is assumed that this formation is partially derived from original structure of the precursor while further disintegration of such particle leads to smaller crisps of irregular shape shown around. Irregular particles with flat surface show sharp edges as noted in Fig. 4(b). In addition, sparse round holes are visible on the surface at magnification of 2000 times. Such holes are openings of the large pores which are significant for diffusion of adsorbate through the structure of the solid.

3.4. Wet chemistry techniques

Boehm's titrations, pH$_{PZC}$ and pH of LVC were employed in a try to elucidate the acid–base character of the LVC surface. Undoubtedly, carbonization followed by activation of the precursor involves introduction of acidic functional groups in the structure of the final material. From the Boehm's titrations it
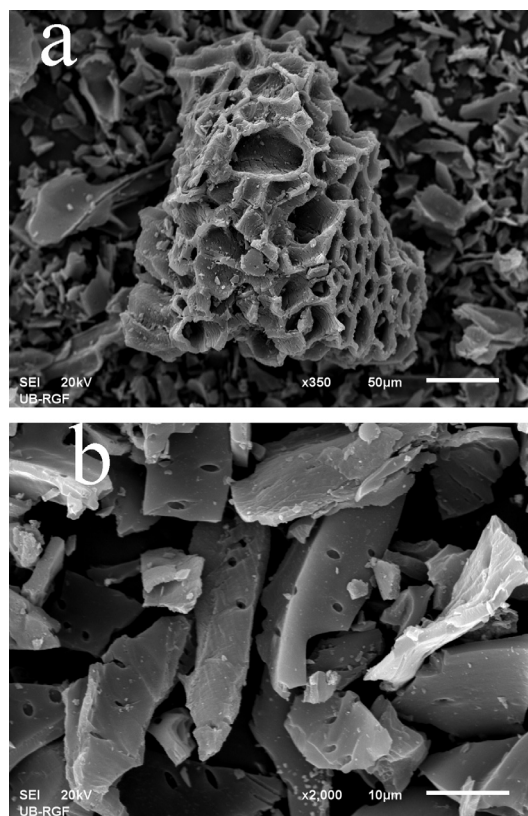

Figure 4 SEM micrographs of the LVC at (a) 350 and (b) 2000 times magnifications.

can be concluded that very acidic groups such as carboxylic make almost 50% of all acidic groups in the analyzed sample. The inferior presence of less acidic lactone groups was detected by neutralization with Na$_2$CO$_3$. As measured by pH of LVC, acidic groups of LVC are in water suspensions well balanced with basic moieties giving response close to neutral pH value. pH$_{PZC}$ determined by drift method evidenced the same conclusions about neutral nature of LVC surface (see Table 2).

3.5. Adsorption kinetics

The applicability of the pseudo-first-order, pseudo-second-order model, Elovich model, and intraparticle diffusion model has been tested for the adsorption of ranitidine onto LVC. Used equations of these models are available in paper by Momčilović et al. (2014).

Ranitidine evidenced very fast adsorption kinetics with reaching the climax of the process in about an hour (Fig. 5).

Table 2 Results of Boehm titrations, pH$_{PZC}$ and pH of LVC.

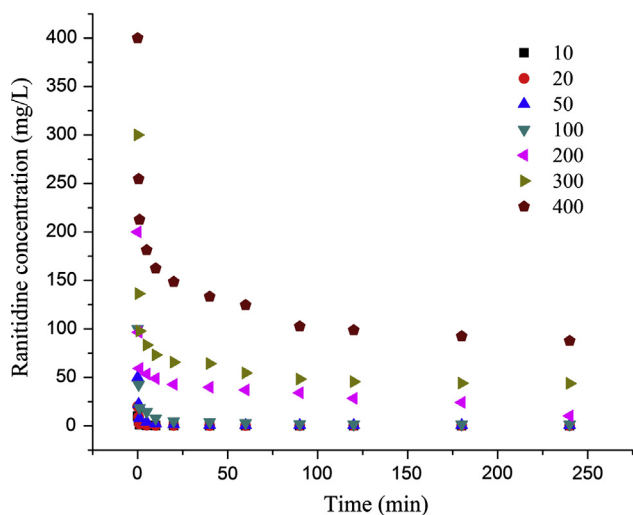| Type of functional groups on LVC (µeq/g)	Value
Acidic groups neutralized by NaHCO$_3$	64
Weakly acidic groups neutralized by Na$_2$CO$_3$	40
Very weakly acidic groups neutralized by NaOH	140
pH$_{PZC}$	7.2
pH	6.6

Figure 5 Kinetics of ranitidine adsorption (initial concentrations from 10 to 400 mg dm^{-3}).

Adsorption capacity rises quickly in the first minutes of the contacting and after the first hour it goes up minimally until equilibrium is formally attained. It depicts readiness of LVC to bind substrates from the aqueous phase.

Fittings to four kinetic models were done for all initial concentrations in order to find out if the suitability of the certain model changes in different cases. Pseudo-second order model gave the best correlation coefficients in any case. This model implies sharing of electrons between the adsorbate and the surface of the adsorbent. Theoretically calculated q_{max} value by this model is close to experimental value.

Adsorption is generally envisioned as a multistage process starting with approaching of adsorbate to the adsorbent surface which is the fastest adsorption stage followed by intra-particle diffusion (a delayed process) and the third stage which includes diffusion through smaller pores, followed by establishment of equilibrium (Cardoso et al., 2011). Interestingly, by rising initial concentrations fittings to Elovich and intra-particle diffusion model showed strong increase of correlation coefficients confirming that, then, the process is controlled by the diffusion of the adsorbate in the pores of the LVC as the slowest step. In this case, adsorption kinetics is influenced by

the speed of ranitidine penetration through the porous structure of LVC (see Table 3).

3.6. Influence of pH

The influence of solution pH onto kinetics of ranitidine adsorption is depicted in Fig. 6. At various pH values adsorption kinetics follows the same trend since removal degrees from pH 2 toward pH 11 changed from 93% to 99%, respectively. Hence, it can be noticed that adsorption is moderately favored at higher pH values presumably influenced by the strong interactions at the carbon–drug interface. The simple reason for such behavior might be a positive charge on nitrogen atoms of ranitidine due to protonation (Fig. 1). Namely, ranitidine hydrochloride used herein is present in the solution as the protonated molecule which is positively charged. This is further responsible for electrostatic repulsions with positively charged carbon surface in acidic solution. As pH rises adsorbent surface becomes more negative and enables unobstructed binding. Similar conclusion is found for ranitidine adsorption onto cellulose (Bezerra et al., 2014).
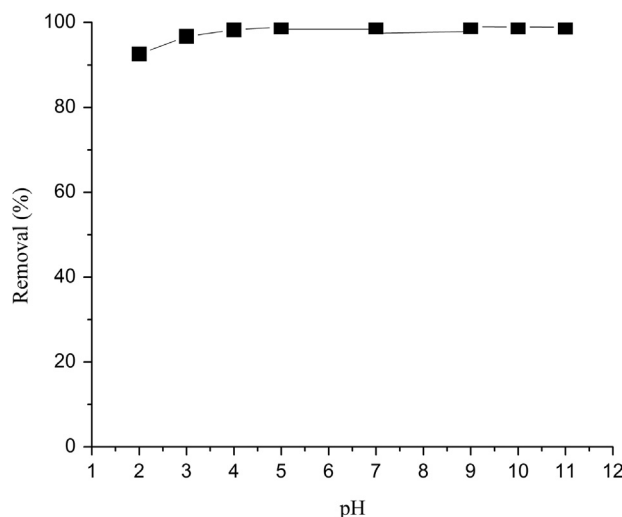

Figure 6 Influence of pH onto ranitidine adsorption.

Table 3 Comparison for kinetic parameters for adsorption of ranitidine onto LVC.

Model	Constant	10 mg/L	20 mg/L	50 mg/L	100 mg/L	200 mg/L	300 mg/L	400 mg/L
Pseudo-first order	q_e (mg/g)	0.71	0.57	1.47	17.53	90.02	36.27	76.71
	k_1 (g/mg min)	0.066	0.031	0.016	0.049	0.025	0.014	0.011
	r^2	0.775	0.591	0.631	0.946	0.805	0.915	0.931
Pseudo-second order	q_e (mg/g)	9.95	19.92	49.5	98.81	189.03	257.73	317.46
	k_2 (g/mg min)	0.843	0.317	0.075	0.015	0.001	0.002	0.001
	r^2	1	1	1	0.999	0.997	0.999	0.999
Elovich	α (mg/g min)	$1.9 \cdot 10^9$	$3.9 \cdot 10^6$	$7.1 \cdot 10^7$	$2.8 \cdot 10^4$	$1.6 \cdot 10^6$	$6.9 \cdot 10^7$	$4.2 \cdot 10^4$
	β (g/mg)	2.7	0.962	0.443	0.164	0.095	0.081	0.042
	r^2	0.436	0.487	0.598	0.781	0.881	0.913	0.974
Intra-particle	k_i (g/mg min)	0.048	0.345	0.547	2.673	3.665	3.569	6.151
	r^2	0.088	0.192	0.255	0.5	0.771	0.626	0.698

Slight pH rises during adsorption experiments, less than one unit, were noticed only for pH 3–5. Out of this range, pH values remained constant throughout all experiments. Such behavior is ascribed to the neutral nature of the LVC. Namely, since pH of LVC was determined to be 6.6 and pH$_{PZC}$ 7.2, this material spontaneously interacts with solution after suspending and rises its pH.

3.7. Adsorption isotherms

The obtained equilibrium data (Fig. 5) were fitted to several theoretical isotherm models including Langmuir, Freundlich and Temkin model. The original equations are presented in detail in paper by Hameed et al. (2007). Using the linear equations written below, corresponding plots were made and linearly fitted using OriginPro 8.0 (OriginLab Corporation, USA) in order to estimate which model fits the actual data best (see Table 4).

The fitting results showed the best correlation with Langmuir isotherm model. This model implies monolayer adsorption where all adsorption cites are homogenous and bind adsorbate molecules with the same adsorption energies. In addition, no lateral interaction and steric hindrance between the adsorbed molecules are anticipated (Momčilović et al., 2013).

Value for q_{max} estimated by Langmuir model is 317.4 mg/g while experimentally determined value is q_{exp} = 315.5 mg/g. Such values are much higher than maximum adsorption capacities obtained in the case of similar experiments involving natural cellulose as adsorbent (q_{exp} = 23.4 mg/g) (Bezerra et al., 2014) and superheated steam activated carbon derived from mung bean husk (q_{max} = 28.0 mg/g) (Mondala et al., 2014).

The value of separation factor (R_L) indicates the type of the isotherm and the nature of the adsorption process. Considering the R_L value, adsorption can be unfavorable ($R_L > 0$), linear ($R_L = 1$), favorable ($0 > R_L > 1$) or irreversible ($R_L = 0$) (Karagoz et al., 2008). In our work, separation factor falls between 0 and 1 and indicates favorable adsorption.

3.8. The effect of adsorbent dose

The optimal adsorbent dosage was examined (Fig. 7). Initial ranitidine concentration of 50 mg/L dropped in the first hour significantly with the rule that more adsorbent mass induces
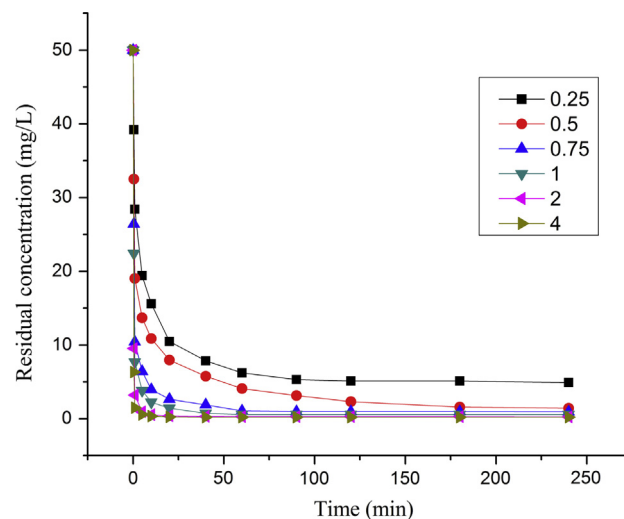

Figure 7 The effect of initial LVC dose (0.25, 0.5, 0.75, 1, 2, and 4 g/L).

more rapid removal. However, from Fig. 8 where removal degree is displayed, can be seen that the optimal dosage is around 1 g/L since further increase in adsorbent mass does not result in further removal in considerable degree. In accordance with this, this dosage is picked for all experiments. The conclusion is that this dose is enough for more than 99% removal of dissolved ranitidine, while the rest remains in the solution as a result of dynamic adsorption–desorption equilibrium. Mondala et al., 2014 faced similar trend when superheated steam activated carbon derived from mung bean husk showed maximum removal of around 95% at dosage of 1 g/L for initial ranitidine concentration of 100 mg/L.

3.9. Thermodynamic parameters

The Gibbs free energy changes ($\Delta G°$) for adsorption in the case of different initial concentrations were calculated according to the following thermodynamic equations:

$$\Delta G° = -RT \ln K_d \tag{3}$$

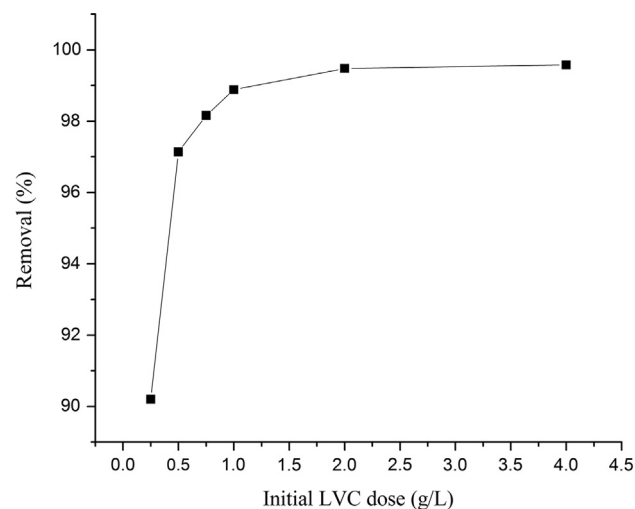**Table 4** Isotherm parameters for adsorption of ranitidine onto LVC.

Model	Constant	Value
Langmuir	K_L (L/g)	84.745
	α_L (L/mg)	0.267
	q_{max} (mg/g)	317.39
	R_L	$2.9 \cdot 10^{-5}$
	r^2	0.987
Freundlich	K_F ((mg/g) (1/mg)$^{1/n}$)	51.82
	n	2.227
	r^2	0.948
Temkin	K_T (L/mg)	12.55
	B	41.27
	r^2	0.959

Figure 8 Optimal adsorbent dosage for ranitidine removal.

Table 5 The Gibbs free energy changes ($\Delta G°$) at 25 °C.

C_i (mg/L)	$\Delta G°$ (kJ/mol)
10	−13.11
20	−12.88
50	−11.29
100	−10.42
200	−7.26
300	−4.46
400	−3.26

where R (8.314 J/mol K) is the perfect gas constant, T is the solution temperature (K) and K_d the distribution coefficient calculated as:

$$K_d = \frac{C_{ads}}{C_{rem}} \quad (4)$$

where C_{ads} is the amount of ranitidine adsorbed at equilibrium (mg/L), and C_{rem} is the concentration of ranitidine remaining in the solution at equilibrium (mg/L).

Calculated values are given in Table 5. It is established that the $\Delta G°$ value is in the range from 0 to −20 kJ/mol and from −80 to −400 kJ/mol for physical and chemical adsorption, respectively (Guedidi et al., 2017). In our case, physical adsorption is implied. According to this, the mechanism of ranitidine removal from solution does not involve any chemical rearrangements nor bond cleavages but only electrostatic, ionic and dipole interactions with the LVC porous structure. Namely, it is well established that carboxylic, carbonylic, lactonic, phenolic, aldehydic groups are present at the edges of hexagonal layer planes of activated carbon microstructure (Bandosz and Ania, 2006). Such groups in deprotonated form are responsible for electrostatic attractions with positively polarized ranitidine molecule across its three N-atoms. In addition, physical capture of adsorbates within tunnel-like LVC structure is expected since we previously described pores with wall thickness of 2.2 nm. Meso- and micropore wall dimensions are suitable for adsorbate retaining in the solid matrix of carbon.

The negative $\Delta G°$ value indicates feasibility and spontaneous nature of adsorption while rising initial drug concentrations give less negative $\Delta G°$ values. Increase in $\Delta G°$ values with initial ranitidine concentrations indicates that the adsorption becomes more favorable.

3.10. Economical aspects

Although popular options for activated carbon production based on coconut shell, coals and wood provide high adsorption capacities for wide range of adsorbates, developing possibilities for cheaper alternatives is still in need. Activated carbon present on the market in the powdered and granular form has value between 600 and 2000 USD/t on average. *L. vulgaris* shell which is used herein as a precursor for the production of superior carbon adsorbent is considered as extremely economical resource since its production costs are minimal. This plant is grown with no special demands, uses of pesticides and expensive agricultural procedures. Further thermo-chemical conversion to final carbon product comprises only of costs of a few cheap chemicals and electric energy used for heating. So, final cost of obtained carbon is estimated to less than 500 USD/t which make it very interesting in the light of its commercialization and practical usage in the future.

4. Conclusion

Employed procedure for carbonization and steam activation of *L. vulgaris* shell gave a carbon material with well developed microporosity, diverse morphology and strong adsorption affinity toward omnipresent drug ranitidine. Lignin and cellulose groups of the precursor have taken the most prominent role in the developing of neutral nature of the LVC surface along with formation of acidic function groups. Noticed neutral response in water suspension is a result of well balanced acidic and basic groups on the LVC surface.

Fast adsorption of ranitidine was observed. Experimental data suggested best fit in the case of Langmuir and pseudo-second order model. A rather good accordance of experimental (315.5 mg/g) and theoretical (317.4 mg/g) values for maximum adsorption capacity was evidenced. These results are much better than the results presented in similar studies regarding ranitidine removal. This implies monolayer adsorption onto energetically homogenous active centers. Transfer of adsorbate mass through the channeled structure of adsorbate appeared to be influenced by the initial ranitidine concentration. Calculated Gibbs free energy changes ($\Delta G°$) indicate spontaneous nature of the process. Adsorption is hindered in acidic solution due to strong electrostatic repulsions between positively charged molecule of drug and highly protonated carboxylic, alcohol, and lactone groups located at the LVC surface.

It is expected that the collected data will be useful for designing thought-out adsorption scheme for efficient ranitidine removal from aqueous solutions. Moreover, easy and economical conversion route for the *L. vulgaris* shell benefited in novel meaningful options for application of this plant.

References

Aljeboree, A.M., Alshirifi, A.N., Alkaim, A.F., 2017. Kinetics and equilibrium study for the adsorption of textile dyes onto coconut shell activated carbon. Arab. J. Chem. 10, S3381–S3393. http://dx.doi.org/10.1016/j.arabjc.2014.01.020. Available at: < http://www.researchgate.net/publication/260030257_Kinetics_and_equilibrium_study_for_the_adsorption_of_textile_dyes_onto_coconut_shell_activated_carbon > .

Aziz, A., Ouali, M.S., Elandaloussi, E.H., Menorval, L.C.D., Lindheimer, M., 2009. Chemically modified olive stone: a low-cost sorbent for heavy metals and basic dyes removal from aqueous solution. J. Hazard. Mater. 163, 441–447.

Addamo, M., Augugliaro, V., Paola, A.D., Garcia-lopez, E., Loddo, V., Marci, G., Palmisano, L., 2005. Removal of drugs in aqueous systems by photoassisted degradation. J. Appl. Electrochem. 35, 765–774.

Bezerra, R.D.S., Silva, M.M.F., Morais, A.I.S., Santos, M.R.M.C., Airoldi, C., Filho, E.C.S., 2014. Natural cellulose for ranitidine drug removal from aqueous solutions. J. Environ. Chem. Eng. 2, 605–611.

Bandosz, T.J., Ania, C.O., 2006. Surface chemistry of activated carbons and its characterization. In: Bandosz, T., Activated Carbon Surfaces in Environmental Remediation, Elsevier, p. 160.

Barrett, E.P., Joyner, L.G., Halenda, P.P., 1951. The determination of pore volume and area distributions in porous substances. I. Computations from nitrogen isotherms. J. Am. Chem. Soc. 73, 373–380.

Brunauer, S., Emmett, P.H., Teller, E., 1938. Adsorption of gases in multimolecular layers. J. Am. Chem. Soc. 60, 309–319.

Cabrita, I., Ruiz, B., Mestre, A.S., Fonseca, I.M., Carvalho, A.P., Ania, C.O., 2010. Removal of an analgesic using activated carbons prepared from urban and industrial residues. Chem. Eng. J. 163, 249–255.

Cardoso, N.F., Pinto, R.B., Lima, E.C., Calvete, T., Amavisca, C.V., Royer, B., Cunha, M.L., Fernandes, T.H.M., Pinto, I.S., 2011. Removal of remazol black B textile dye from aqueous solution by adsorption. Desalination 269, 92–103.

Cazetta, A.L., Vargas, A.M., Nogami, E.M., Kunita, M.H., Guilher-me, M.R., Martins, A.C., Silva, T.L., Moraes, J.G., Almeida, V.C., 2011. NaOH-activated carbon of high surface area produced from coconut shell: kinetics and equilibrium studies from the methylene blue adsorption. Chem. Eng. J. 174, 117–125.

Castiglioni, S., Bagnati, R., Fanelli, R., Pomati, F., Calamari, D., Zuccato, E., 2006. Removal of pharmaceuticals in sewage treat-ment plants in Italy. Environ. Sci. Technol. 40, 357–363.

Decker-Walters, D.S., Wilkins-Ellert, M., Chung, S.M., Staub, J.E., 2004. Discovery and genetic assessment of wild bottle gourd from Zimbabwe. Econ. Bot. 58, 501–508.

El Khames Saad, M., Khiari, R., Elaloui, E., Moussaoui, Y., 2014. Adsorption of anthracene using activated carbon and *Posidonia oceanic*. Arab. J. Chem. 7, 109–113.

Fernandez, M.E., Nunell, G.V., Bonelli, P.B., Cukierman, A.L., 2014. Activated carbon developed from orange peels: batch and dynamic competitive adsorption of basic dyes. Ind. Crop. Prod. 62, 437–445.

Fukahori, S., Fujiwara, T., Ito, R., Funamizu, N., 2011. PH-dependent adsorption of sulfa drugs on high silica zeolite: modeling and kinetic study. Desalination 275, 237–242.

Figueroa, R.A., Leonard, A., Mackay, A.A., 2004. Modeling tetracy-cline antibiotic sorption to clays. Environ. Sci. Technol. 38, 476–483.

González, P.G., Pliego-Cuervo, Y.B., 2014. Adsorption of Cd(II), Hg(II) and Zn(II) from aqueous solution using mesoporous activated carbon produced from *Bambusa vulgaris striata*. Chem. Eng. Res. Des. 92, 2715–2724

Guedidi, H., Reinert, L., Soneda, Y., Bellakhal, N., Duclaux, L., 2017. Adsorption of ibuprofen from aqueous solution on chemically surface-modified activated carbon cloths. Arab. J. Chem. 10, S3584–S3594. http://dx.doi.org/10.1016/j.arabjc.2014.03.007.

Ghule, B.V., Ghante, M.H., Saoji, N., Yeole, P.G., 2009. Antihyperlip-idemic effect of the methanolic extract from *Lagenaria siceraria* Stand. fruit in hyperlipidemic rats. J. Ethnopharmacol. 124, 333–337.

Hameed, B.H., Ahmad, A.L., Latiff, K.N.A., 2007. Adsorption of basic dye (methylene blue) onto activated carbon prepared from rattan sawdust. Dyes Pigm. 75, 143–149.

Jones, O.A.H., Voulvoulis, N., Lester, J.N., 2005. Human pharma-ceuticals in wastewater treatment processes. Crit. Rev. Environ. Sci. Technol. 35, 401–427.

Kyzas, G.Z., Kostoglou, M., Lazaridis, N.K., Lambropoulou, D.A., Bikiaris, D.N., 2013. Environmental friendly technology for the removal of pharmaceutical contaminants from wastewaters using modified chitosan adsorbents. Chem. Eng. J. 222, 248–258.

Karagoz, S., Tay, T., Ucar, S., Erdem, M., 2008. Activated carbons from waste biomass by sulfuric acid activation and their use on methylene blue adsorption. Bioresour. Technol. 99, 6214–6222.

Momčilović, M.Z., Ranđelović, M.S., Onjia, A.E., Zarubica, A., Babić, B.M., Matović, B.Z., 2013. Study on efficient removal of

clopyralid from water using resorcinol-formaldehyde carbon cryo-gel. J. Serb. Chem. Soc. 79, 481–494.

Momčilović, M.Z., Ranđelović, M.S., Purenović, M., Onjia, A.E., Babić, B.M., Matović, B.Z., 2014. Synthesis and characterization of resorcinol formaldehyde carbon cryogel as efficient sorbent for imidacloprid removal. Desalination Water Treat. 52, 7306–7316.

Mondala, S., Sinha, K., Aikat, K., Halder, G., 2014. Adsorption thermodynamics and kinetics of ranitidine hydrochloride onto superheated steam activated carbon derived from mung bean husk. J. Environ. Chem. Eng. http://dx.doi.org/10.1016/j.jece.2014.11.021.

Menendez-Diaz, J.A., Martin-Gullon, I., 2006. Types of carbon adsorbents and their production. In: Bandosz, T., Activated Carbon Surfaces in Environmental Remediation, Elsevier, p. 12.

Mitić-Stojanović, D.L., Bojić, D., Mitrović, J., Andjelković, T., Radović, M., Bojić, A., 2012. Equilibrium and kinetic studies of Pb(II), Cd(II) and Zn(II) sorption by *Lagenaria vulgaris* shell. Chem. Ind. Chem. Eng. Quat. 18, 563–576.

Narayana, B., Veena, K., Ashwani, K., Shetty, D.N., 2010. New reagents for the spectrophotometric determination of ranitidine hydrochloride. Ecletica Química. 35 (3), 109–115.

Obregón-Valencia, D., Rosario Sun-Kou, M., 2014. Comparative cadmium adsorption study on activated carbon prepared from aguaje (*Mauritia flexuosa*) and olive fruit stones (*Olea europaea* L.). J. Environ. Chem. Eng. 2, 2280–2288.

Ofomaja, A.E., Naidoo, E.B., 2010. Biosorption of lead(II) onto pine cone powder: studies on biosorption performance and process design to minimize biosorbent mass. Carbohydr. Polym. 82, 1031–1042.

Pfaffen, V., Ortiz, P.I., 2010. Alternative method with amperometric detection for ranitidine determination. Ind. Eng. Chem. Res. 49, 4026–4030.

Prahas, D., Kartika, Y., Indraswati, N., Ismadji, S., 2008. Activated carbon from jackfruit peel waste by H_3PO_4 chemical activation: pore structure and surface chemistry characterization. Chem. Eng. J. 140, 32–42.

Qin, C., Chen, Y., Gao, Y., 2014. Manufacture and characterization of activated carbon from marigold straw (*Tagetes erecta* L) by H_3PO_4 chemical activation. Mater. Lett. 135, 123–126.

Rutherford, D.W., Wershaw, R.L., Cox, L.G., 2005. Changes in Composition and Porosity Occurring During the Thermal Degra-dation of Wood and Wood Components – Scientific Investigations Report 2004-5292. U.S. Geological Survey, Reston, Virginia.

Rouquerol, F., Rouquerol, J., Sing, K., 1999. Adsorption by Powders and Porous Solids. Academic Press, London, UK, p. 111.

Sires, I., Brillas, E., 2012. Remediation of water pollution caused by pharmaceutical residues based on electrochemical separation and degradation technologies: a review. Environ. Int. 40, 212–229.

Salleha, M.A.M., Mahmoud, D.K., Karim, W.A.W.A., Idris, A., 2011. Cationic and anionic dye adsorption by agricultural solid wastes: a comprehensive review. Desalination 280, 1–13.

Salve, P., Gharge, D., Kirtawade, R., Dhabale, P., Burade, K., 2010. Simple validated spectroscopic method for estimation of ranitidine from tablet formulation. Int. J. Pharm Tech Res. 2 (3), 2071–2074.

Vediappan, K., Lee, C.W., 2011. Electrochemical approaches for the determination of ranitidine drug reaction mechanism. Curr. Appl. Phys. 11, 995–1000.

Wu, L., Zhang, X., Liu, D., Peng, H., Long, T., 2014. Activated carbons derived from livestock sewage sludge and their absorption ability for the livestock sewage. IERI Procedia 9, 33–42.

Xu, J., Chen, L., Qu, H., Jiao, Y., Xie, J., Xing, G., 2014. Preparation and characterization of activated carbon from reedy grass leaves by chemical activation with H_3PO_4. Appl. Surf. Sci. 320, 674–680.

Youssef, A.M., El-Nabarawy, T., Samra, S.E., 2004. Sorption prop-erties of chemically-activated carbons: 1. Sorption of cadmium(II) ions. Colloid Surf. A 235, 153–163.